REFERENCE 152

R. L. OLCOTT, "HOMOGENEOUS HEAVY WATER MODERATED CRITICAL ASSEMBLIES, PART I, EXPERIMENTAL," NUCL. SCI. ENG. 1: 327-341 (1956).

THE JOURNAL OF THE AMERICAN NUCLEAR SOCIETY

NUCLEAR SCIENCE and ENGINEERING

Volume 1, 1956

ACADEMIC PRESS INC., PUBLISHERS, NEW YORK 3, N. Y.

Homogeneous Heavy Water Moderated Critical Assemblies. Part 1. Experimental

RICHARD N. OLCOTT[1]

Los Alamos Scientific Laboratory, Los Alamos, New Mexico

Received March 14, 1956

Ten critical assemblies of enriched uranyl-fluoride heavy-water solutions have been studied. In six cases, heavy water reflectors surrounded solutions in which the atomic ratio of deuterium to uranium-235 varied from 34 to 430. The remaining four assemblies were without reflector and the deuterium to U^{235} ratio ranged from 230 to 2080. Activation rates within the systems were measured for the resonance detectors In, Au, Pd, and Mn and for the fission detectors U^{235}, U^{238}, Pu^{239}, and U^{233}.

INTRODUCTION

Because of the interest in reactors with epithermal neutron spectra, flexible assembly machines were designed to permit measurements upon critical heavy water solution systems (at room temperature) over a wide range of deuterium to U^{235} atomic ratios. In addition to measurements for calibration purposes, pile periods in the absence of delayed neutrons, and fission detector and resonance detector activations were determined for these assemblies. The study of fission and resonance response constituted the major portion of the experiments, with the aim of establishing some of the neutron spectral characteristics.

DESCRIPTION OF CRITICAL MACHINES AND MATERIAL

SPHERES WITH D_2O REFLECTOR

Figure 1 is a diagram of the equipment for solution spheres with heavy water reflector. The main components of the assembly are a reflector storage reservoir, a pumping system to transfer the reflector between the reservoir and a 35-in. diameter stainless steel sphere, and (centered in the reflector sphere) any of a series of stainless steel spherical shells for various concentrations of $U^{235}O_2F_2$-D_2O solution. The D_2O reflector container is fixed at 35 in. diameter; therefore, the reflector thickness decreases with increased size of active solution sphere. Diameters of these 0.040-in. wall spheres ranged from 13.5 to 18.5 in.

[1] Now with Westinghouse Electric Corporation, Atomic Power Division, Pittsburgh, Pennsylvania.

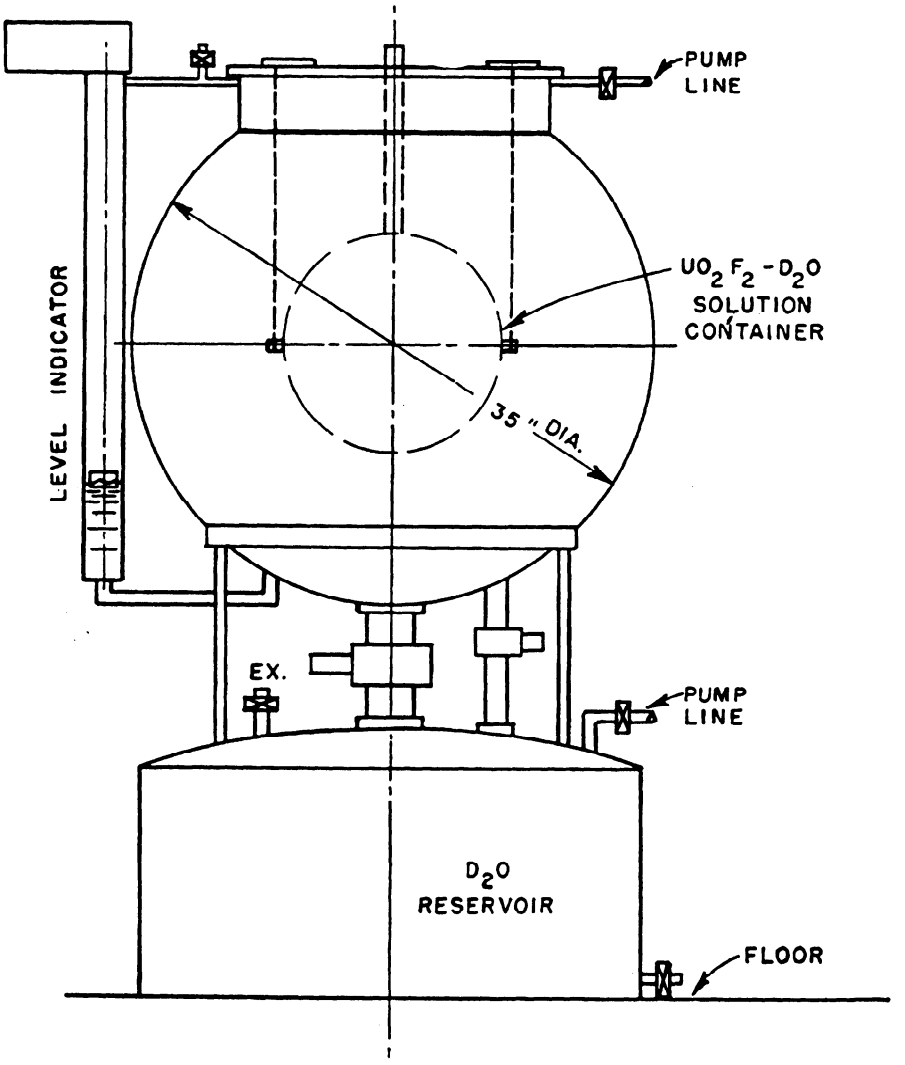

FIG. 1. Schematic drawing of reflected UO_2F_2-D_2O system.

UNREFLECTED CYLINDERS

A diagram of the arrangements for cylindircal solutions without reflector, is shown in Fig. 2. The storage reservoir, in which the $U^{235}O_2F_2$-D_2O solution is kept when the assembly is not operating, is of annular design to limit neutron multiplication for personnel safety. There is a pumping system for transferring the active solution from the storage annulus to the stainless steel reactor cylinder. Two reactor cylinders of 25 and 30 in. diameter were available so that the active solution height would not differ greatly from its diameter at any delayed critical measurement within the concentration range of interest.

MATERIAL

The isotopic concentration of deuterium in the reflector ranged from an initial 99.8% to about 99.0% at the end of the series. This change probably resulted

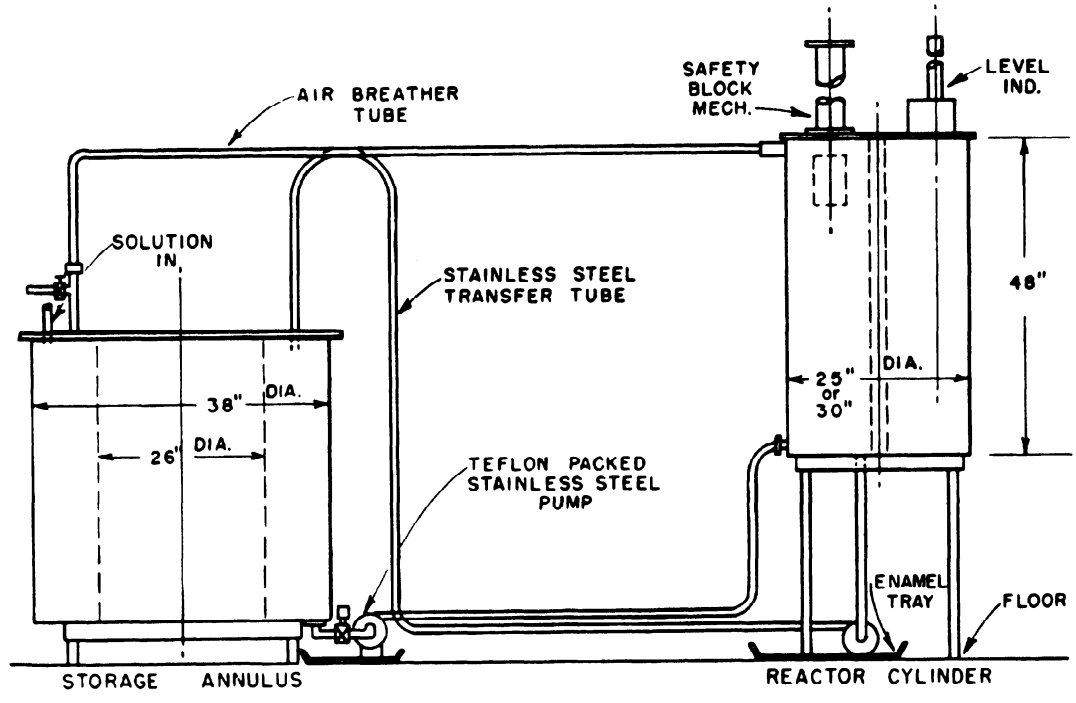

FIG. 2. Schematic drawing of bare $U^{235}O_2F_2$ systems.

from exchange with atmospheric water vapor. The purity of heavy water in the solutions is discussed later. Uranium densities of the solutions at various concentrations were determined by chemical analyses. The uranium was approximately 90% U^{235}.

DETERMINATION OF DELAYED CRITICAL

To follow neutron multiplication during buildup toward critical, four external boron-lined neutron counters in long geometry (*1*) were directed towards the center of the reactor tank. A neutron source in a stainless steel source holder was located in the center of the reactor. For each sphere, increments of a concentrated master solution of D_2O were added in quantities which the preceding measurements indicated were necessary to approach critical with the sphere full and reflector complete. The D_2O reflector was pumped into location by remote operation. Control near delayed critical was by means of small adjustments in the reflector level.

In the case of the bare system, increasing quantities of solution of the desired concentration were transferred (by remote control) from the storage annulus to the reactor cylinder until the critical volume was attained. Changes in solution level served as control near delayed critical.

DELAYED CRITICAL PARAMETERS

Table I gives the delayed critical conditions observed with the series of $U^{235}O_2F_2$-D_2O solutions reflected with D_2O. Where necessary, slight corrections

TABLE I

DELAYED CRITICAL DATA FOR SPHERICAL $U^{235}O_2F_2$-D_2O SOLUTIONS IN D_2O REFLECTOR

Sphere diameter (inches)	Critical volume (liters)	Critical mass (kg U^{235})	D/U^{235} atomic ratio	U^{235} density (gm/cm³)	D_2O reflector thickness (inches)
13.5	20.9	14.2	34.2	0.679	10.7
14.5	26.1	11.6	53.7	0.443	10.2
15.5	31.7	9.6	81.2	0.302	9.7
16.5	38.1	7.0	135.3	0.185	9.2
17.5	45.9	4.8	243	0.104	8.7
18.5	53.8	3.2	431	0.060	8.2

TABLE II

DELAYED CRITICAL DATA FOR BARE CYLINDRICAL $U^{235}O_2F_2$-D_2O SOLUTIONS. (CONTAINER ⅛ IN. STAINLESS STEEL)

Observed data

D/U^{235} atomic ratio	U^{235} density (gm/cm³)	Cyl. inside radius (cm)	Axial glory hole	Critical height (cm)	Critical volume (liters)
230	0.1094	31.6	1-in. o.d.-s.s.	71.45	223.8
419	0.0610	31.6	1-in. o.d.-s.s.	78.74	246.6
856	0.0301	38.1	1-in. o.d.-s.s.	61.09	278.0
856	0.0301	38.1	1⅛-in. o.d.-Al	60.83	276.8
2081	0.0124	38.1	1⅛-in. o.d.-Al	84.75	385.8

Reduced data

D/U^{235} atomic ratio	Cyl. critical radius (cm) glory hole removed	Cyl. critical volume (liters) glory hole removed	Critical volume of sphere in ⅛-in. s.s. (liters)[a]	Critical volume of ideal bare sphere (liters)[a]	Critical mass of bare sphere (kg U^{235})
230	31.55	223.1	194.4	197.7	21.6
419	31.53	245.5	208.2	211.7	12.9
856	38.04	275.9	243.3	247.0	7.4
2081	38.04	384.6	335.4	340.1	4.2

[a] Assumes equivalent stainless steel thickness of 0.2 cm, extrapolation distance of 2.5 cm (critical volume is increased 1.1 to 1.2% for extrapolation distance of 3.9 cm). There has been no correction for ~1 *a/o* H^1 contamination of the D in these solutions. (Ed. note: *a/o* = atomic per cent, *w/o* = weight per cent.)

were applied to the measured critical volumes to normalize them to a critical reflector level 17.5 in. above center. Table II gives the delayed critical data for the unreflected assemblies, and the results of reduction to spherical shape. Figure 3 shows the spherical critical volumes and critical masses as functions of D/U^{235} atomic ratios for both reflected and unreflected assemblies. From the overlapping portions of the sets of curves, that is, within the D/U^{235} range of 230 to 420, it is seen that the critical mass with an ~8½-in. thick D_2O reflector is about one-quarter that of the corresponding bare assembly.

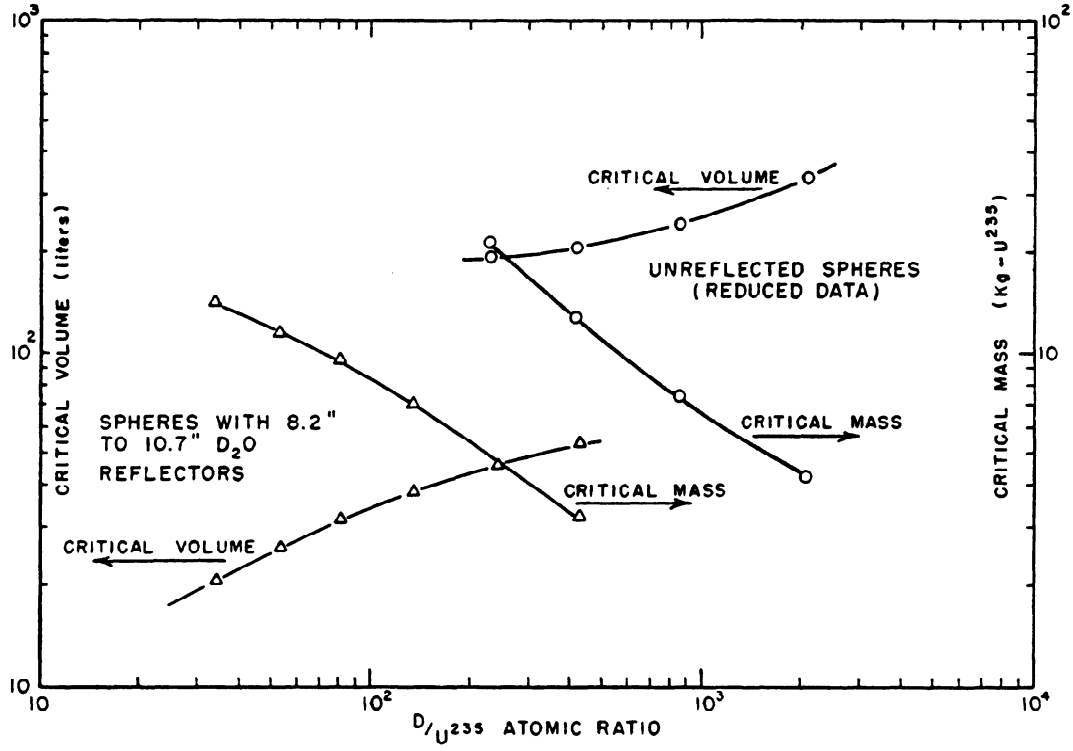

FIG. 3. Spherical critical volume and critical mass as function of D/U^{235} atomic ratio for the $U^{235}O_2F_2$-D_2O solution assemblies.

CHARACTERISTICS ESTABLISHED BY VARIOUS EXPERIMENTS

The principal emphasis of the experimental program with critical $U^{235}O_2F_2$-D_2O systems was on information to help understand neutron behavior in the U^{235} "resonance region." This section treats a few supplementary types of measurement that were included.

NEUTRON AGE IN D_2O

The age in heavy water (99.8%) of neutrons approximating a fission spectrum was determined by activation of cadmium-covered indium detectors, roughly one mean-free-path thick for resonance neutrons (1.44 ev). Measurements were made at various distances from an enriched uranium sphere, which had a neutron multiplication of about eight when placed at the center of the 35-in. diameter sphere of heavy water. The distribution of activity is given in Fig. 4. In D_2O the neutron age thus determined is 111 ± 1 cm^2, as compared with 100 ± 5 cm^2 in "The Reactor Handbook, Vol. I, Physics," p. 485 (*2*).

EXAMPLE OF CALIBRATION MEASUREMENTS

Positive periods were measured for control calibration of the assembly with the 13.5-in. diameter sphere in D_2O reflector. The periods were obtained at a series of reflector levels and interpreted by means of the inhour relation and delayed neutron data of Keepin and Wimett (*3*) to give values of excess re-

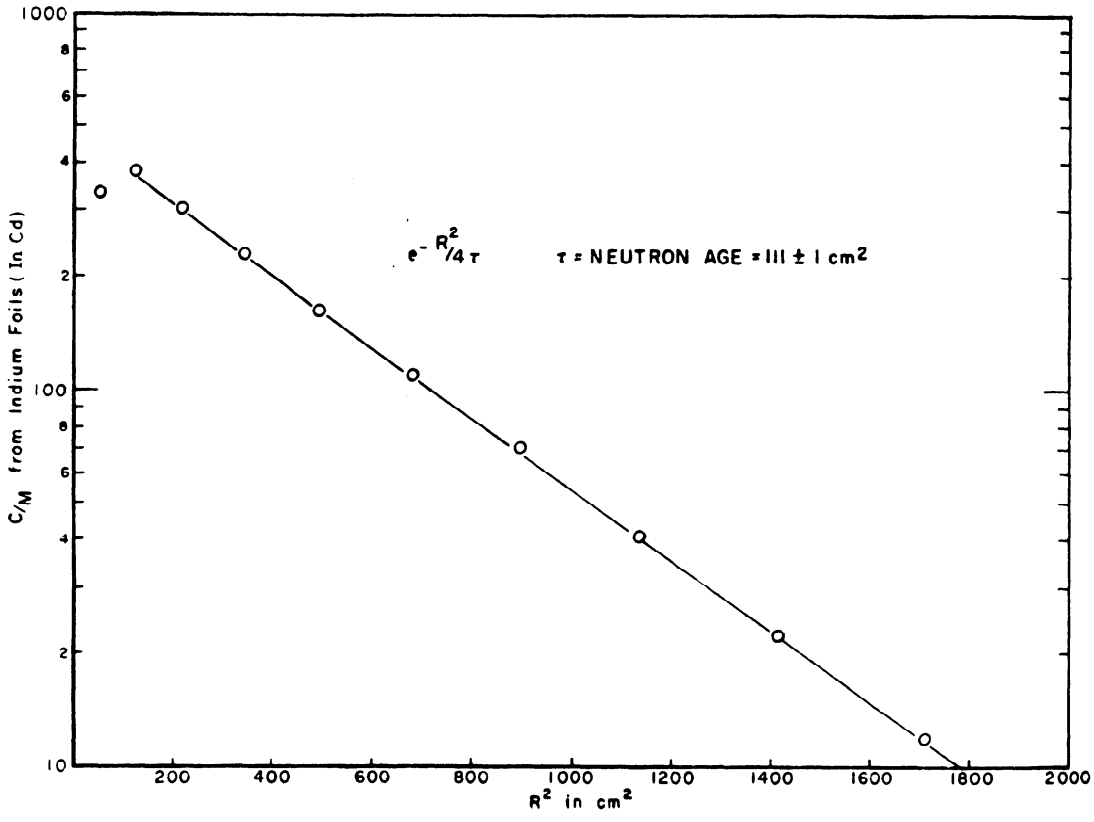

FIG. 4. Specific activity of cadmium-covered indium foils in D_2O as a function of distance from a fission neutron source.

activity in cents (100 cents is the interval between delayed and prompt critical). The reflector level range so calibrated overlapped a region over which recriprocal multiplication values had been determined (with active material reduced slightly). From curves ΔK (cents) and $1/M$ *versus* D_2O level, one finds that a change of reactivity of 100 cents corresponds to a change of reciprocal multiplication of 0.015.

PERIODS IN THE ABSENCE OF DELAYED NEUTRONS

Values of Rossi[2] alpha, the reciprocal period that a multiplying assembly would have in the absence of delayed neutrons, were determined for one assembly. Within the range of interest, Rossi alpha is a linear function of reactivity that becomes zero at prompt critical. Measurements on the spherical assembly at $D/U^{235} = 34.2$ gave a value of -476 sec^{-1} at a multiplication of 16.5 and -177 sec^{-1} at a multiplication of 68.8. Using the value 0.015 for $\Delta(1/M)$ corresponding to 100 cents, an average value of Rossi alpha at delayed critical of -90 ± 10 sec^{-1} is obtained. For comparison, the corresponding value for a metal assembly is $-380{,}000$ sec^{-1} (*4*), indicating the much shorter prompt neutron lifetime in the metal assembly.

[2] Named for Bruno Rossi, who developed techniques for measuring this quantity while he was at Los Alamos.

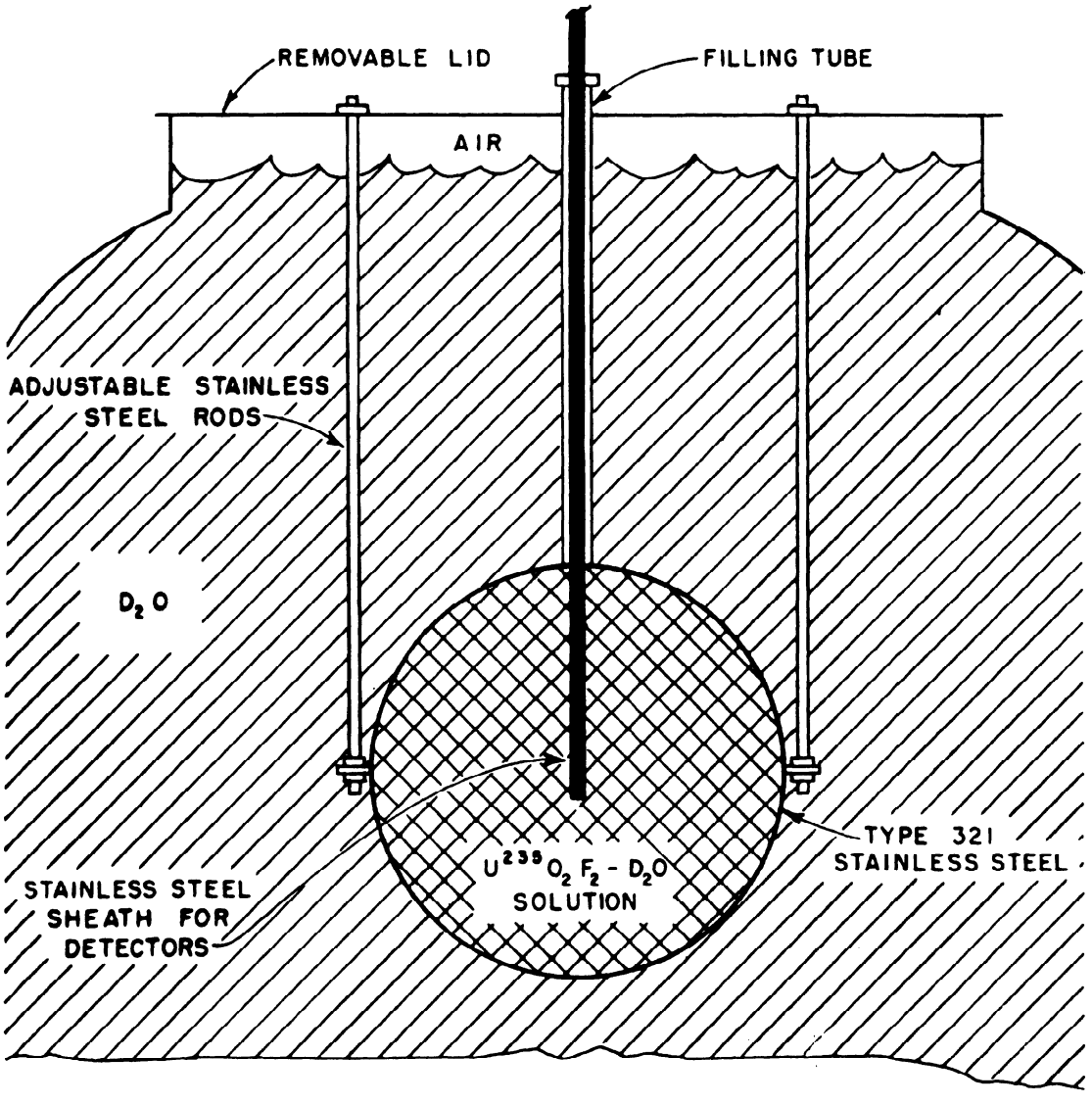

FIG. 5. Solution sphere with sheath for detectors.

SPECIFIC ACTIVITIES OF FISSION AND RESONANCE DETECTORS

Responses of various detectors were determined in both types of geometry. In each reflected assembly the "glory hole" for containing detectors was a removable stainless steel sheath extending through the filling tube of the solution sphere to the center. Figure 5 shows the location of the sheath for the placing of detectors. For the various spheres there were differences in height of active solution in the filling tubes, and also variations in D_2O reflector level, which introduced local distortions of detector response. In the bare assemblies the "glory hole" was a fixed axial cylinder that extended through the solution. Type 321 stainless steel "glory hole" cylinders used initially in these assemblies were later replaced by aluminum because of the concern over absorption by the steel. In both the reflected and unreflected systems, the detector holder was a thin brass strip with milled recesses to locate a series of detectors at 1.5-in. intervals.

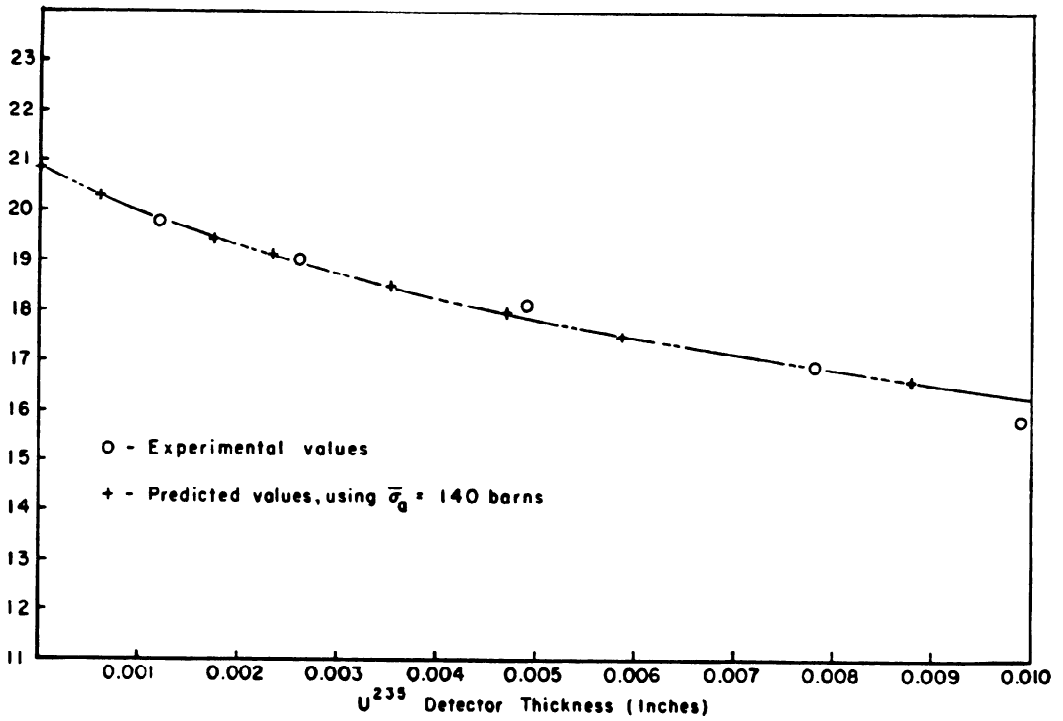

FIG. 6. Specific activity of U^{235} detectors of various thicknesses at the center of 18.5-in. diameter sphere. $D/U^{235} = 431$.

FISSION DETECTORS

For the assemblies with D_2O reflector, U^{235} detectors, with and without cadmium, were irradiated at various radii, and activities determined by counting the fission product gammas. Such measurements yield directly the power distribution within the core, and less directly, a resolution of the total flux for both core and reflector into two neutron energy components or groups separated by the cadmium "cut-off" energy ($\sim$0.6 ev).

Because of the large thermal cross section of U^{235}, it was necessary to determine the extent of neutron self-shielding in the standard 0.005-in. thick foils. This was accomplished by irradiating a series of foils of different thicknesses. As an example, Fig. 6 shows how the specific activity varied with thickness of bare U^{235} detectors in the 18.5-in. diameter solution sphere. As a guide for the extrapolation to zero thickness, we have used the known dependence of specific absorption on foil thickness for the simple case where the foil responds to an isotropic flux exposure nvt, with a unique absorption cross section σ_a, and scattering is negligible:

$$\text{spec. abs. (per gram)} = N\sigma_a(nvt)\,\frac{1 - e^{-x}(1 - x) - x^2[-\mathrm{Ei}(-x)]}{2x}$$

where N is the number of foil atoms/gm, $-\mathrm{Ei}(-x)$ is the logarithmic integral of x as defined by Jahnke-Emde the foil thickness expressed in mean free paths

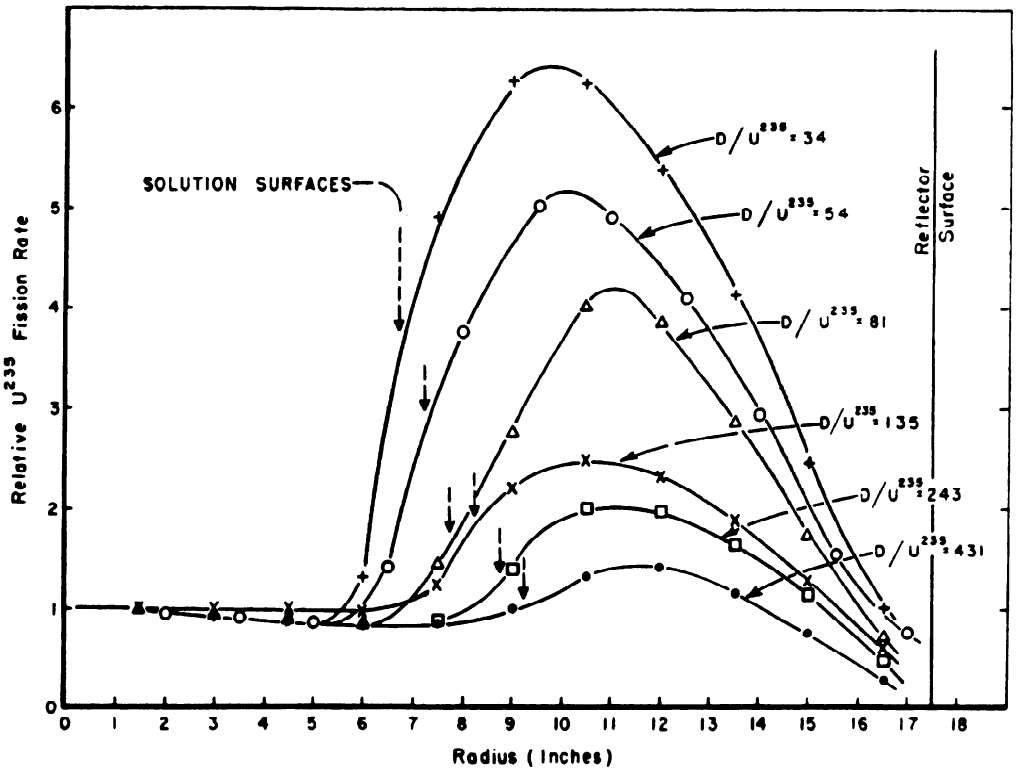

FIG. 7. Bare 0.005-in. U^{235} detector response as a function of radius in the D_2O reflected systems. Active solution was high in filling tube of 15.5-in. diameter sphere.

For large x, the foil diameter should be small compared to the neutron mean free path in the surrounding medium. The best fit of the U^{235} data to this equation occurs for $\sigma_a = 140$ barns.

Figure 7 shows the dependence upon radius of the specific activity of bare 0.005-in. U^{235} detectors for the various concentrations of U^{235} in the reflected assemblies. Figure 8 gives the U^{235} cadmium ratio as a function of position for the 13.5- and 18.5-in. diameter spheres, and lists central values for all spheres.

In the unreflected assemblies, gamma-counting data from U^{235}, U^{238}, and Pu^{239} detectors were supplemented by central measurements with small, multiple fission chambers containing thin foils of U^{235}, U^{238}, U^{233}, Pu^{239}, and Np^{237}. Axial variations followed the expected cos kh relationship, where h is the distance from center. Results from the central fission chambers and comparisons with data from gamma-counted fission detectors are listed in Table III. In this table, $\bar{\sigma}_f$ is the effective cross section for the spectrum studied and is defined by the following relation:

$$\bar{\sigma}_f = \frac{\int_0^\infty \sigma_f(E)\phi(E)\,dE}{\int_0^\infty \phi(E)\,dE}$$

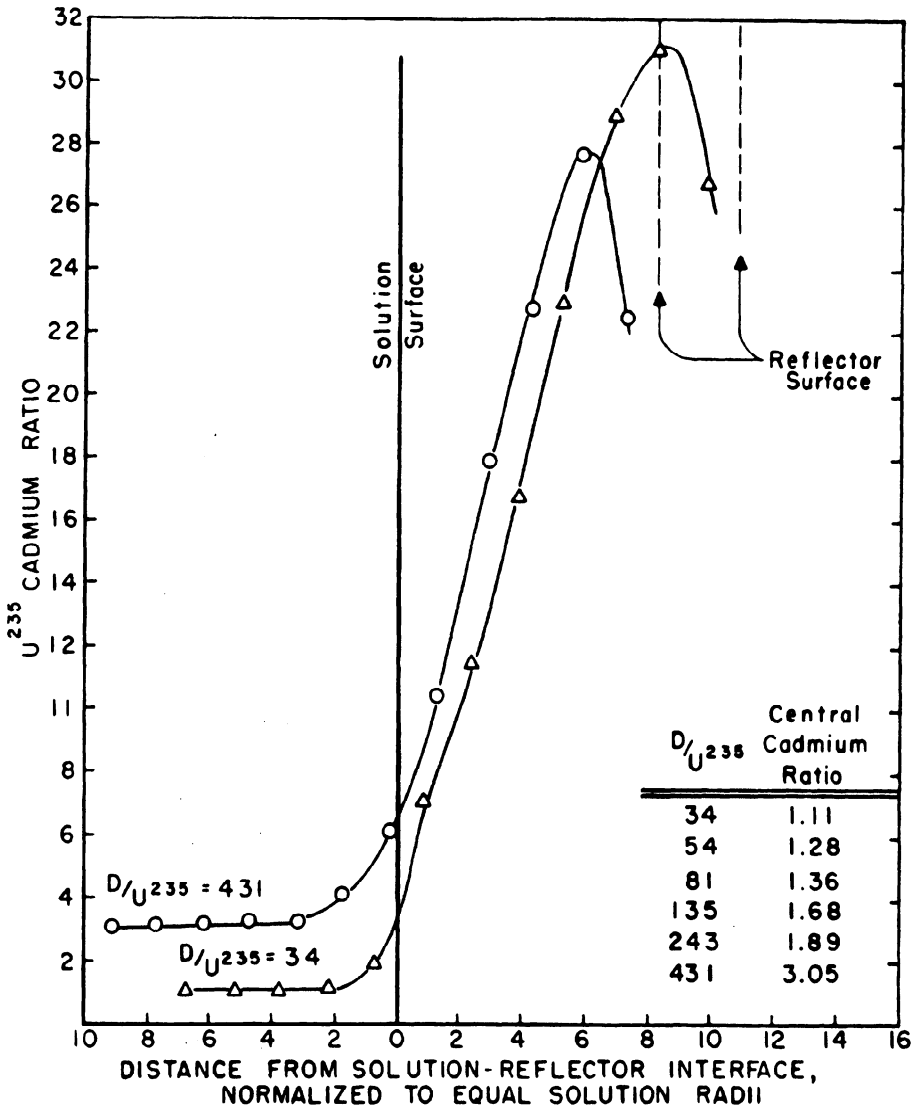

FIG. 8. U^{235} cadmium ratio as a function of position in the 13.5- and 18.5-in. diameter spheres, D_2O reflected; 0.005-in. thick U^{235} and 0.032-in. thick cadmium.

where $\phi(E)$ is the flux of neutrons of energy E, expressed as neutrons per cm^2 per unit energy interval per unit time, and $\sigma_f(E)$ is the fission cross section of the detector at energy E.

As an illustration of how these additional fission detectors further characterize the solution spectra or, what is equivalent, permit resolution of total flux into neutron groups, we give the following reduction of the central values of $\bar{\sigma}_f(U^{235})/\bar{\sigma}_f(U^{238})$ and the cadmium ratio CR (U^{235}) for the assembly at $D/U^{235} = 856$. Letting the fraction of the total flux consisting of neutrons with energies under the cadmium cut-off energy ($\sim$0.6 ev) be designated ϕ_1, that fraction between the cadmium cutoff and the U^{238} fission threshold ($\sim 1.4 \times 10^6$ ev) be designated

TABLE III

CENTRAL SPECTRAL INDICES IN UNREFLECTED $U^{235}O_2F_2$-D_2O SOLUTIONS

Spectral indices	$D/U^{235} = 230$		$D/U^{235} = 856$	$D/U^{235} = 2110$	
	Fission chamber[a]	Product γ counting[b]	Fission chamber[a]	Fission chamber[a]	Product γ counting[b]
$\overline{\sigma_f}(Pu^{239})/\overline{\sigma_f}(U^{235})$	3.05	2.96	2.52	2.03	1.93
$\overline{\sigma_f}(U^{233}/\overline{\sigma_f}(U^{235})$	1.78		1.29	1.11	
$\overline{\sigma_f}(U^{235})/\overline{\sigma_f}(U^{238})$	384	379	1123	3180	3075
$\overline{\sigma_f}(Np^{237})/\overline{\sigma_f}(U^{238})$	4.13		3.59		
$\overline{\sigma_f}(U^{235})/\overline{\sigma_f}(U^{235}$ in 17 mil Cd)	2.01		4.79	10.6	
$\overline{\sigma_f}(U^{235})/\overline{\sigma_f}(U^{235}$ in 32 mil Cd)		1.99		12.4	11.5
$\overline{\sigma_f}(Pu^{239})/\overline{\sigma_f}(Pu^{239}$ in 17 mil Cd)	3.60		5.59	11.61	
$\overline{\sigma_f}(Pu^{239})/\overline{\sigma_f}(Pu^{239}$ in 32 mil Cd)		3.82		15.8	18.5
$\overline{\sigma_f}(U^{233})/\overline{\sigma_f}(U^{233}$ in 17 mil Cd)	1.43		2.51	11.5	

[a] Foil weights from 1 μg to 200 μg; areas about 0.3 cm^2.

[b] Values extrapolated to zero detector thickness.

as ϕ_2, and the remaining fraction above the U^{238} fission threshold be designated ϕ_3, one has

$$\frac{\overline{\sigma_f}(U^{238})}{\overline{\sigma_f}(U^{235})} = \frac{\sigma_{f3}(U^{238})\phi_3}{\sigma_{f1}(U^{235})\phi_1 + \sigma_{f2}(U^{235})\phi_2 + \sigma_{f3}(U^{235})\phi_3}$$

$$CR(U^{235}) = \frac{\sigma_{f1}(U^{235})\phi_1 + \sigma_{f2}(U^{235})\phi_2 + \sigma_{f3}(U^{235})\phi_3}{\sigma_{f2}(U^{235})\phi_2 + \sigma_{f3}(U^{235})\phi_3}$$

and

$$1 = \phi_1 + \phi_2 + \phi_3$$

where $\sigma_{fn}(x)$ is the response or cross section of detector x for neutrons in the nth energy group. With the approximate values (and herein lies a major difficulty for proper data reduction), $\sigma_{f3}(U^{238}) \sim 0.5$ barn, $\sigma_{f1}(U^{235}) \sim 500$ barns, $\sigma_{f2}(U^{235}) \sim 20$ barns, and $\sigma_{f3}(U^{235}) \sim 1.3$ barns, one obtains $\phi_1 \sim 0.116$, $\phi_2 \sim 0.754$, and $\phi_3 \sim 0.130$.

It may be noted (Table III) that at $D/U^{235} = 2110$ the Pu^{239} cadmium ratio is more sensitive to cadmium thickness change from 0.017 in. to 0.032 in. than is the U^{235} ratio. This difference is consistent with expected incomplete shielding of the 0.3-ev Pu^{239} resonance by the overlapping cadmium resonance.

RESONANCE DETECTORS

Specific activities of indium, gold, palladium, and manganese were obtained at various axial positions as functions of foil thickness, with and without cadmium, in both types of assembly. These five detectors have large neutron resonances in the 1–300 ev range, and, if there is sufficient absorption in these res-

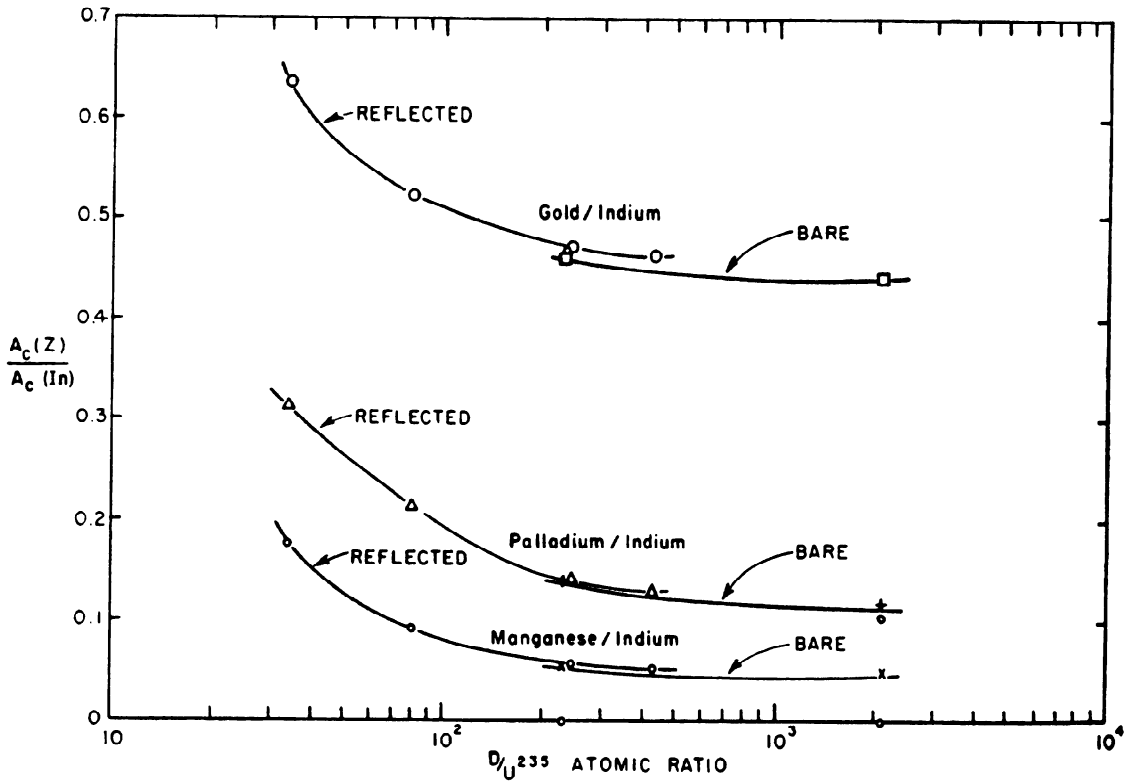

FIG. 9. Central response ratios of cadmium-covered resonance detectors.

onances, responses in the different assemblies would help to determine the corresponding spectral shapes in this energy region. Because the average neutron energy decreases with increasing D/U^{235} atomic ratio, the thermal contribution of the specific activity increasingly masks resonance effects. To emphasize contributions in the resonance region, central activation ratios for cadmium covered detectors are given in Fig. 9 as a function of D/U^{235} atomic ratio for both bare and reflected assemblies. It is apparent that the influence of reflector on the central spectrum is minor. The response of cadmium-coated foil (A_C) still contains, in addition to the response from resonance neutron absorption, a contribution due to the absorption of other epithermal and fast neutrons. To determine this nonresonance contribution, the responses ($A_{C,NR}$) were measured for foils sandwiched between additional 0.005-in. foils of the same material and covered with 0.032-in. cadmium. The outer foils act as shields against the resonance neutrons and, as an operational definition of resonance response, A_R, we shall use $A_R = A_C - A_{C,NR}$. Central values of bare foil activities (A_0), A_C, $A_{C,NR}$, and A_R are listed in Table IV for $D/U^{235} = 230$ and 2110. The results $A_R \sim 0$ for manganese indicate that there is no significant resonance capture. This is consistent with the report of Seidl *et al.* (*5*) that 340-ev resonance of Mn is primarily a scattering phenomenon.

The use of A_R values to characterize epithermal spectra may be illustrated

TABLE IV

RESONANCE DETECTOR RESPONSES—BARE SOLUTIONS. SPECIFIC ACTIVITIES NORMALIZED TO RESPONSE OF AU MONITOR

Detector and principal resonance	Foil thickness (mg/cm²)	A_0 Total response (bare foil)	A_C Nonthermal response (Cd-shielded foil)	$A_{C,NR}$ Nonresonance response (Cd + self-shielded foil)	A_R Resonance response ($A_C - A_{C,NR}$)
		$D/U^{235} = 230$			
In (1.44 ev)	20	98.5	83.8	21.6	62.2
Au (4.9 ev)	23	42.2	38.6	9.3	29.3
Pd (34 ev)	10	12.2	11.7	3.0	8.7
Mn (340 ev)	29	7.4	4.7	3.9	0.8
		$D/U^{235} = 2110$			
In (1.44 ev)	20	81.3	40.8	9.8	31.0
Au (4.9 ev)	23	33.3	18.0	4.4	13.6
Pd (34 ev)	10	6.3	4.8	1.3	3.5
Mn (340 ev)	29	13.3	2.0	2.0	0.0

crudely. First, it is expected that the flux in the solution at $D/U^{235} = 2110$ is nearly "flat," that is, uniform per logarithmic energy interval. In this case,

$$\phi'(E_Z)/\phi'(E_{In}) = kA'_R(Z)/A'_R(In) = 1$$

where $\phi(E_Z)$ is the flux per logarithmic energy interval at the principal resonance of the element Z, and the In resonance is simply a convenient reference. Now, for the spectrum at $D/U^{235} = 230$,

$$\phi(E_Z)/\phi(E_{In}) = kA_R(Z)/A_R(In) = [A_R(Z)/A_R(In)]/[A'_R(Z)/A'_R(In)].$$

Inserting values of A_R from Table IV, we have the approximate flux ratios:

$$\phi(E_{Au})/\phi(E_{In}) = \phi(4.9 \text{ ev})/\phi(1.44 \text{ ev}) \sim 1.07$$

$$\phi(E_{Pd})/\phi(E_{In}) = \phi(34 \text{ ev})/\phi(1.44 \text{ ev}) \sim 1.24.$$

DISCUSSION OF RESULTS

ERRORS

It is estimated that errors of values of critical volume are less than ±1% for the existing conditions, and that errors of corresponding U^{235} concentrations or D/U^{235} ratios are within ±2%. For the reflected systems, the standard solution and D_2O levels to which critical volumes were adjusted, were selected to compensate roughly for the effect of the filling tube channel through the reflector and for asphericity of the outer reflector surface.

The critical systems were nonideal in two principal respects. First, neutron absorption by the stainless steel solution spheres in the reflected assemblies is

estimated to increase critical volumes a maximum of ~2% above values for nonabsorbing containers. The second effect is that of normal water contamination of the D_2O solutions (other contaminants were minor and the reflector contamination by normal water is of slight significance). In the spherical solutions, the hydrogen was probably between 99.6 and 99.8 atomic per cent D, and the main effect of the normal hydrogen is an increase in moderation. The correction to pure D_2O corresponds to ~1% critical volume increase at nominal D/U^{235}. The large-volume cylindrical solutions contained D_2O which had been incompletely protected against water vapor. Spot checks suggest that the normal hydrogen contamination averaged roughly 1 atomic per cent. In this case, the correction to pure D_2O, is a 2–3% increase in critical volume at nominal D/U^{235}.

There is at present no convincing basis for assigning errors to absolute values of specific absorption; relative values, however, apparently have probable errors about ±3%. Actually, absolute values are of little utility because of the imperfect knowledge of detector cross sections, and relative values are sufficient to give information about spectral differences (see previous examples).

Problems Requiring Detailed Theoretical Treatment

A primary function of a set of detector responses is the elucidation of flux spectra for reactive assemblies or regions of reactive assemblies (1) which are too complex to compute in a time or with an accuracy competitive with experiment or (2) for which the cross sections characterizing the reactive media are inadequately known. For the comparatively simple assemblies discussed here, accurate computational techniques are available and considerable effort has been made during the past decade to obtain accurate U^{235} cross sections over most of the energy range below ~3 Mev.

For these assemblies, the weakness in theoretical flux spectra due to remaining uncertainties in material cross sections (for example, in the U^{235} (n, γ) cross section in the epithermal region) must be pitted against the weakness of the experimental spectral information due to the limited number of available detectors and uncertainties in their response characteristics (for example, uncertainties in the nature of secondary resonances in the case of resonance detectors). A theoretical program, now under way, will attempt to answer which of the two methods of spectral determinations is the more accurate for these assemblies and to what extent the two methods supplement one another. In this comparison of methods, the critical mass data afford necessary check points for the theoretical calculations.

Acknowledgment

I wish to mention some of the people responsible for major portions of the work to which I have referred—a list of all who contributed would be too lengthy. The first and major

phases of the engineering design and construction were due to Glen A. Newby. To G. A. Linenberger I would like to give personal thanks for guidance and advice during the initial portion of the investigation, and to George A. Jarvis for his excellent work with the small, multiple foil fission chambers, which he designed. I would like to pay special tribute to Gordon E. Hansen and Hugh C. Paxton for their theoretical advice and review of this report.

REFERENCES

1. A. O. HANSEN and J. L. MCKIBBEN, *Phys. Rev.* **72,** 673-677 (1947).
2. "The Reactor Handbook: Vol. 1, Physics" U. S. Atomic Energy Commission Doc. AECD-3645 or McGraw-Hill, New York, 1955.
3. G. R. KEEPIN and T. F. WIMETT, Geneva Conference Paper No. 831 (1955).
4. R. H. WHITE, *Nuclear Sci. and Eng.* **1,** 53-61 (1956).
5. F. G. P. SEIDL, D. J. HUGHES, H. PALEVSKY, J. S. LEVIN, W. Y. KATO, and N. G. SJÖSTRAND, *Phys. Rev.* **95,** 476-499 (1954).